

Chapter 1

MAMMA: a 1-D steady state model of volcanic conduits

MAMMA (Magma Ascent Mathematical Modeling and Analysis) is a FORTRAN90 code designed to solve a conservative model for steady magma ascent in a volcanic conduit, described as a compressible multicomponent two-phase flow. It is an open-source code (<https://github.com/demichie/MAMMA>) mainly developed by Mattia de'Michieli Vitturi. This document has been redacted by Alvaro Aravena Ponce.

1.1 System of equations

The system of conservation equations is derived from the theory of thermodynamically compatible systems [1], considering the effects of the main processes that magmas experience during ascent, such as crystallization, rheological changes, fragmentation, injection of external water, physical interaction with conduit walls, outgassing and degassing. The system is described as a mixture of two phases ($i = 1, 2$), each one characterized by a volumetric fraction (α_i), density (ρ_i), velocity (u_i) and specific entropy (s_i). Below the fragmentation level, phase 1 is a mixture of crystals, dissolved water and melt (continuous phase); while phase 2 is composed by the exsolved gas bubbles (dispersed phase). Above magma fragmentation, phase 1 is constituted by magma fragments (dispersed phase) and phase 2 is the exsolved gas mixture (continuous phase). Magma

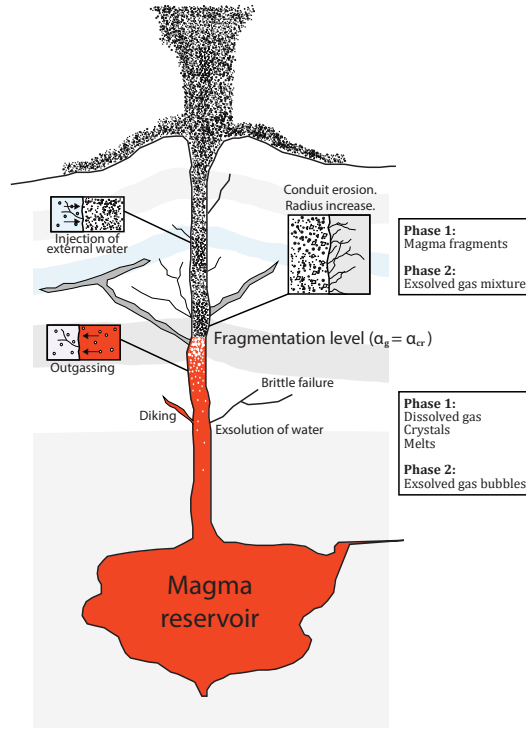


FIGURE 1.1: Schematic illustration of volcanic conduits.

fragmentation occurs when the exsolved gas volumetric fraction reaches a critical value ($\alpha_g = \alpha_{cr}$) [2] (Fig. 1.1).

The components of the system are characterized by an equation of state; while pressure (p_i) and temperature (T_i) of both phases are derived from the internal energy (e_i):

$$p_i = \rho_i^2 \frac{\partial e_i}{\partial \rho_i} \quad (1.1)$$

$$T_i = \frac{\partial e_i}{\partial s_i} \quad (1.2)$$

The model is capable of describing conduits with elliptical cross sections, and it includes the conservation laws of total mass (Eq. 1.3), momentum (Eq. 1.4) and energy (Eq. 1.5).

$$\frac{\partial}{\partial z} \left(\rho u R_{eq}^2 \right) = 2J_{ex} f_{\epsilon_1} R_{eq} - 2J_{lat} f_{\epsilon_1} R_{eq} \quad (1.3)$$

$$\begin{aligned} \frac{\partial}{\partial z} \left(\left(\alpha_1(\rho_1 u_1^2 + p_1) + \alpha_2(\rho_2 u_2^2 + p_2) \right) R_{eq}^2 \right) \\ = -\rho g R_{eq}^2 - 2J_{lat} f_{\epsilon_1} u_2 R_{eq} - \frac{8\chi_1 \mu u_1}{f_{\epsilon_2}^2} - \frac{\chi_2 \lambda_w \rho_2 u_2^2 R_{eq}}{4f_{\epsilon_2}^2} \end{aligned} \quad (1.4)$$

$$\begin{aligned} \frac{\partial}{\partial z} \left(\left(\alpha_1 \rho_1 u_1 \left(e_1 + \frac{p_1}{\rho_1} + \frac{u_1^2}{2} \right) + \alpha_2 \rho_2 u_2 \left(e_2 + \frac{p_2}{\rho_2} + \frac{u_2^2}{2} \right) \right. \right. \\ \left. \left. - \rho x_1 x_2 (u_1 - u_2)(s_1 - s_2) T \right) R_{eq}^2 \right) = -\rho g u R_{eq}^2 - \frac{8\chi_1 \mu u_1^2}{f_{\epsilon_2}^2} \\ - \frac{\chi_2 \lambda_w \rho_2 u_2^3 R_{eq}}{4f_{\epsilon_2}^2} + 2J_{ex} f_{\epsilon_1} c_w T_w R_{eq} - 2J_{lat} f_{\epsilon_1} \left(c_g T + \frac{u_2^2}{2} \right) R_{eq} \end{aligned} \quad (1.5)$$

where z is the vertical coordinate, ρ is mixture density, u is mixture velocity, R_{eq} is the equivalent conduit radius (Eq. 1.6), J_{ex} is the mass flux of external water, f_{ϵ_1} is a conduit eccentricity-derived factor (Eq. 1.7), J_{lat} is the lateral gas flux through conduit walls, g is the acceleration of gravity, χ_i controls the inclusion of wall friction contribution (1 or 0, function of the continuous phase index), μ is mixture viscosity, f_{ϵ_2} is an additional conduit eccentricity-derived factor (Eq. 1.8), λ_w is a drag coefficient [3], x_i is the mass fraction of phase i , T is mixture temperature, c_w is the specific heat capacity of external water, T_w is the external water temperature and c_g is the specific heat capacity of exsolved water.

$$R_{eq} = \sqrt{R_a \cdot R_b} \quad (1.6)$$

$$f_{\epsilon_1} = \frac{3(1 + \sqrt{1 - \epsilon^2}) - \sqrt{(3 + \sqrt{1 - \epsilon^2}) \cdot (1 + 3\sqrt{1 - \epsilon^2})}}{2 \cdot \sqrt[4]{1 - \epsilon^2}} \quad (1.7)$$

$$f_{\epsilon_2} = \sqrt{\frac{2\sqrt{1 - \epsilon^2}}{2 - \epsilon^2}} \quad (1.8)$$

where ϵ is conduit eccentricity (Eq. 1.9), R_a is the maximum semi-axis and R_b is the minimum semi-axis.

$$\epsilon = \sqrt{1 - \frac{R_b^2}{R_a^2}} \quad (1.9)$$

Phase 1 volume fraction is governed by the following equation:

$$\frac{\partial}{\partial z} \left(\rho u \alpha_1 R_{eq}^2 \right) = -\frac{1}{\tau(p)} (p_2 - p_1) R_{eq}^2 \quad (1.10)$$

where $\tau^{(p)}$ is the relaxation parameter which controls the pressure difference between both phases.

Furthermore, the model includes an additional equation for controlling the relative velocity between phases:

$$\begin{aligned} \frac{\partial}{\partial z} \left(\left(\frac{u_1^2}{2} - \frac{u_2^2}{2} + e_1 - e_2 + \frac{p_1}{\rho_1} - \frac{p_2}{\rho_2} - (s_1 - s_2)T \right) R_{eq}^2 \right) \\ = -\frac{8\chi_1\mu u_1}{\alpha_1\rho_1 f_{\epsilon_2}^2} + \frac{\chi_2\lambda_w u_2^2 R_{eq}}{4\alpha_2 f_{\epsilon_2}^2} - \frac{\rho}{\rho_1\rho_2} \delta_f (u_1 - u_2) R_{eq}^2 \end{aligned} \quad (1.11)$$

where δ_f is the drag factor.

Finally, the system of equations presents the mass conservation laws of crystals (Eq. 1.12), dissolved water (Eq. 1.13) and exsolved gas (Eq. 1.14).

$$\frac{\partial}{\partial z} \left(\alpha_1 \rho_c \alpha_c u_1 R_{eq}^2 \right) = -\frac{1}{\tau^{(c)}} \alpha_1 \rho_c (\alpha_c - \alpha_c^{eq}) R_{eq}^2 \quad (1.12)$$

$$\begin{aligned} \frac{\partial}{\partial z} \left(x_d \alpha_1 (\rho_1 - \alpha_c \rho_c) u_1 R_{eq}^2 \right) \\ = 2J_{ex} f_{\epsilon_1} R_{eq} - \frac{1}{\tau^{(d)}} (x_d - x_d^{eq}) \alpha_1 (\rho_1 - \alpha_c \rho_c) R_{eq}^2 \end{aligned} \quad (1.13)$$

$$\frac{\partial}{\partial z} \left(\alpha_2 \rho_2 u_2 R_{eq}^2 \right) = -2J_{lat} f_{\epsilon_1} R_{eq} + \frac{1}{\tau^{(d)}} (x_d - x_d^{eq}) \alpha_1 (\rho_1 - \alpha_c \rho_c) R_{eq}^2 \quad (1.14)$$

where ρ_c is density of crystals, α_c is the volume fraction of crystals in phase 1, $\tau^{(c)}$ is the crystallization relaxation parameter, α_c^{eq} is the equilibrium value of crystals volume fraction in phase 1, x_d is the mass fraction of dissolved water in the phase composed by melt and dissolved water, $\tau^{(d)}$ is the relaxation parameter which controls the gas exsolution rate, and x_d^{eq} is the equilibrium value of the mass fraction of dissolved water in the phase composed by melt and dissolved water.

When the injection of external water is considered, it is modelled using the following equation [2]:

$$J_{ex} = \frac{\rho_w k_a}{\mu_w f_{\epsilon_2}} \frac{\partial p}{\partial r} \Big|_{r=R_{eq}} \quad (1.15)$$

where ρ_w is external water density, k_a is the aquifer permeability and μ_w is external water viscosity.

For the model solution, it employs a numerical shooting technique: for a given inlet pressure, the model adjusts the inlet flow rate until the appropriate boundary condition (choked flow or atmospheric pressure) is reached. For the spatial integration of the equations, a well-established PI step-size control technique is adopted, with the relaxation terms treated implicitly to guarantee the stability of the numerical scheme.

1.2 Constitutive equations

In order to offer the possibility of describing the behaviour of a wide range of magma compositions and volcanic phenomena, a complete set of constitutive equations has been implemented in the code.

1.2.1 Viscosity models

Since it has been suggested a strong effect of crystal content [4, 5, 6] and exsolved gas bubbles [6, 7] on the resulting mixture rheology, magma viscosity (μ) is evaluated using the following expression:

$$\mu = \mu_{melt} \cdot \theta_c(\alpha_c) \cdot \theta_g(\alpha_g) \quad (1.16)$$

where μ_{melt} is the crystals and bubbles-free viscosity; whereas $\theta_c(\alpha_c)$ and $\theta_g(\alpha_g)$ account for the effect of crystals and bubbles on the resulting viscosity, respectively.

The following models are implemented for calculating μ_{melt} , while the available expressions for calculating θ_c and θ_g are shown in Tables 1.1 and 1.2, respectively.

Hess and Dingwell [24]

This model is based on a multiple non-linear regression of 111 measurements of viscosity, and is adapted for studying rhyolitic magmas:

$$\log_{10}(\mu_{melt}) = -3.545 + 0.833 \cdot \ln(w) + \frac{9601 - 2368 \cdot \ln(w)}{T - (195.7 + 32.25 \cdot \ln(w))} \quad (1.17)$$

where μ_{melt} is expressed in Pa · s, w is H₂O concentration in wt.% and T is temperature in K.

TABLE 1.1: Available models for calculating $\theta_c(\alpha_c)$ in MAMMA.

| Model | Equation | Auxiliary variables |
|-----------------------|--|---|
| Fixed value | $\theta_c = \theta_{cf}$ | θ_{cf} ⁽¹⁾ |
| Costa [4] | $\theta_c = \left(1 - c_1 \cdot \operatorname{erf}\left(\frac{\sqrt{\pi}}{2} \alpha_c \left(1 + \frac{c_2}{(1-\alpha_c)^{c_3}}\right)\right)\right)^{\frac{c_4}{c_1}}$ | $c_1 = 0.9995$. $c_2 = 1.0$. $c_3 = 1.0$. $c_4 = -2.5$. |
| Dingwell [8] | $\theta_c = \left(1 + 0.75 \cdot \frac{\alpha_c}{c - \alpha_c}\right)^2$ | $c = 0.84$ |
| Lejeune-Richet [9] | $\theta_c = \left(1 - \frac{\alpha_c}{c_1}\right)^{-c_2}$ | $c_1 = 0.7$. $c_2 = 3.4$. |
| Melnik-Sparks v1 [10] | $\log_{10}\left(\frac{\theta_c}{c_1}\right) = \operatorname{atan}(c_2 \cdot (\alpha_c - c_3)) + \frac{\pi}{2}$ | $c_1 = 1.6$. $c_2 = 20.6$. $c_3 = 0.62$. |
| Melnik-Sparks v2 [11] | $\log_{10}\left(\frac{\theta_c}{c_1}\right) = \operatorname{atan}(c_2 \cdot (\alpha_c - c_3)) + \frac{\pi}{2}$ | $c_1 = 1.4$. $c_2 = 8.6$. $c_3 = 0.69$. |
| Vona v1 [12] | $\theta_c = \frac{1 + \phi^{c_2}}{\left(1 - (1 - c_3) \operatorname{erf}\left(\frac{\sqrt{\pi}}{2(1-c_3)} \phi(1 + \phi^{c_4})\right)\right)^{c_1 c_5}}$ | $\phi = \alpha_c / c_1$. $c_1 = 0.27$. $c_2 = 12.16$. $c_3 = 0.032$. $c_4 = 0.84$. $c_5 = 2.8$. |
| Vona v2 [12] | $\theta_c = \frac{1 + \phi^{c_2}}{\left(1 - (1 - c_3) \operatorname{erf}\left(\frac{\sqrt{\pi}}{2(1-c_3)} \phi(1 + \phi^{c_4})\right)\right)^{c_1 c_5}}$ | $\phi = \alpha_c / c_1$. $c_1 = 0.39$. $c_2 = 1.16$. $c_3 = 0.03$. $c_4 = 0.84$. $c_5 = 2.8$. |

⁽¹⁾ Input parameter.TABLE 1.2: Available models for calculating $\theta_g(\alpha_g)$ in MAMMA.

| Model | Equation | Auxiliary variables |
|---------------------------|--|------------------------------------|
| None | $\theta_g = 1.0$ | |
| Bagdassarov-Dingwell [13] | $\theta_g = \frac{1}{1 + b \cdot \alpha_g}$ | $b = 22.4$ |
| Costa et al. [14] | $\theta_g = \frac{1 + 25 \cdot \operatorname{Ca}^2 (1 - \alpha_g)^{8/3}}{(1 - \alpha_g) \cdot (1 + 25 \cdot \operatorname{Ca}^2)}$ | Ca ⁽¹⁾ |
| Ducamp-Raj [15] | $\theta_g = \exp\left(-b \left(\frac{\alpha_g}{1 - \alpha_g}\right)\right)$ | $2.5 < b < 4$ |
| Eilers [16, 17] | $\theta_g = \left(1 + \frac{1.25 \alpha_g}{1 - b \cdot \alpha_b}\right)^2$ | $1.28 < b < 1.30$ |
| Mackenzie [18] | $\theta_g = 1 - \frac{5}{3} \alpha_g$ | |
| Quane-Russel [19] | $\theta_g = \exp\left(\frac{b \cdot \alpha_g}{1 - \alpha_g}\right)$ | $b = -0.63$ ⁽²⁾ |
| Sibree [20] | $\theta_g = \frac{1}{1 - (b \cdot \alpha_g)^{1/3}}$ | $b = 1.2$ |
| Rahaman [21] | $\theta_g = \exp(-b \cdot \alpha_g)$ | $b = 11.2$ |
| Taylor [22] | $\theta_g = 1 + \alpha_g$ | |

⁽¹⁾ Capillarity number. Calculated following Llewellyn and Manga [23].⁽²⁾ Adapted for Phlegrean Fields.

Romano et al. [25]

This model has been calibrated using samples from Vesuvius and Phlegrean Fields. For trachytic magmas, melt viscosity is calculated using:

$$\log_{10}(\mu_{melt}) = -3.5405 + 0.14467 \cdot \ln(w) + \frac{9618.9 - 498.79 \cdot \ln(w)}{T - (191.78 - 35.518 \cdot \ln(w))} \quad (1.18)$$

On the other hand, the following equation is adapted for studying phonolitic magmas:

$$\log_{10}(\mu_{melt}) = -5.8996 - 0.2857 \cdot \ln(w) + \frac{10775 - 394.83 \cdot \ln(w)}{T - (148.71 - 21.65 \cdot \ln(w))} \quad (1.19)$$

Giordano et al. [26]

This model predicts the non-Arrhenian Newtonian viscosity of silicate melts as a function of T and melt composition (major elements). Melt viscosity (μ_{melt}) is calculated using:

$$\log_{10}(\mu_{melt}) = -4.55 + \frac{B_G}{T - C_G} \quad (1.20)$$

where B_G and C_G are composition-dependent constants (Eq. 1.21 and Eq. 1.22, respectively).

$$B_G = \sum_{i=1}^7 (b_i M_i) + \sum_{j=1}^3 b_{1j} M_{1j} \quad (1.21)$$

$$C_G = \sum_{i=1}^6 (c_i N_i) + c_{11} N_{11} \quad (1.22)$$

where M_i , M_{1j} , N_i and N_{11} refer to the combinations of mol% oxides reported in Table 1.3, and b_i , b_{1j} , c_i and c_{11} are constant values (Table 1.3).

Giordano et al. [27]

This model was calibrated using data derived from Stromboli samples, thus it is adapted for studying basaltic magmas. Melt viscosity (μ_{melt}) is determined using the following equation:

TABLE 1.3: Coefficients for calculation of B_G and C_G from melt composition (mol% oxide) [26].

| Coefficient | Value | Oxides |
|-------------|--------|---|
| b_1 | 159.6 | $M_1 = \text{SiO}_2 + \text{TiO}_2$ |
| b_2 | -173.3 | $M_2 = \text{Al}_2\text{O}_3$ |
| b_3 | 72.1 | $M_3 = \text{FeO(T)} + \text{MnO} + \text{P}_2\text{O}_5$ |
| b_4 | 75.7 | $M_4 = \text{MgO}$ |
| b_5 | -39.0 | $M_5 = \text{CaO}$ |
| b_6 | -84.1 | $M_6 = \text{Na}_2\text{O} + \text{V}^{(1)}$ |
| b_7 | 141.5 | $M_7 = \text{V} + \ln(1 + \text{H}_2\text{O})$ |
| b_{11} | -2.43 | $M_{11} = (\text{SiO}_2 + \text{TiO}_2) \cdot (\text{FM}^{(2)})$ |
| b_{12} | -0.91 | $M_{12} = (\text{SiO}_2 + \text{TA}^{(3)} + \text{P}_2\text{O}_5) \cdot (\text{NK}^{(4)} + \text{H}_2\text{O})$ |
| b_{13} | 17.6 | $M_{13} = (\text{Al}_2\text{O}_3) \cdot (\text{NK})$ |
| c_1 | 2.75 | $N_1 = \text{SiO}_2$ |
| c_2 | 15.7 | $N_2 = \text{TA}$ |
| c_3 | 8.3 | $N_3 = \text{FM}$ |
| c_4 | 10.2 | $N_4 = \text{CaO}$ |
| c_5 | -12.3 | $N_5 = \text{NK}$ |
| c_6 | -99.5 | $N_6 = \ln(1 + \text{V})$ |
| c_{11} | 0.30 | $N_{11} = (\text{Al}_2\text{O}_3 + \text{FM} + \text{CaO} - \text{P}_2\text{O}_5) \cdot (\text{NK} + \text{V})$ |

⁽¹⁾ $\text{V} = \text{H}_2\text{O} + \text{F}_2\text{O}_{-1}$.⁽²⁾ $\text{FM} = \text{FeO(T)} + \text{MnO} + \text{MgO}$.⁽³⁾ $\text{TA} = \text{TiO}_2 + \text{Al}_2\text{O}_3$.⁽⁴⁾ $\text{NK} = \text{Na}_2\text{O} + \text{K}_2\text{O}$.

$$\log_{10}(\mu_{melt}) = -4.55 + \frac{6101 - 63.66 \cdot w^*}{T - (567 - 160.3 \cdot \log_{10}(1 + w^*))} \quad (1.23)$$

where w^* is H_2O concentration in mol%.

Whittington et al. [28]

In this case, the viscosity model is adapted to dacitic magmas and uses the following formulation:

$$\log_{10}(\mu_{melt}) = -4.43 + \frac{7618.3 - 17.25 \cdot \log_{10}(w + 0.26)}{T - (406.1 - 292.6 \cdot \log_{10}(w + 0.26))} \quad (1.24)$$

Di Genova et al. [29]

This work includes two viscosity models, adapted for studying the pantelleritic melts from the Khaggiar lava flow. The first formulation (Di Genova v1) uses the parametrization proposed by Giordano et al. [27]:

$$\log_{10}(\mu_{melt}) = -4.55 + \frac{4278.17 + 8.6 \cdot w^*}{T - (513 - 245.3 \cdot \log_{10}(1 + w^*))} \quad (1.25)$$

The second model (Di Genova v2) uses the following parametrization:

$$\log_{10}(\mu_{melt}) = -4.55 + \frac{10528.64 - 4672.21 \cdot \log_{10}(1 + w^*)}{T - (172.27 + 89.75 \cdot \log_{10}(1 + w^*))} \quad (1.26)$$

1.2.2 Solubility models**Henry's law**

The equilibrium value of dissolved water is calculated using the following expression:

$$x_d^{eq} = \sigma \left(\frac{p_g}{1[\text{Pa}]} \right)^\epsilon \quad (1.27)$$

where p_g is pressure of the gas component, σ is the solubility coefficient and ϵ is the solubility exponent.

Polynomial fit

When the polynomial fit is employed, x_d^{eq} is computed with the following expression:

$$x_d^{eq} = c_1 \cdot \left(\frac{p_g}{1[\text{Pa}]} \right)^2 + c_2 \cdot \left(\frac{p_g}{1[\text{Pa}]} \right) \quad (1.28)$$

where c_1 and c_2 are fitting parameters.

Zhang model [30]

In this case, x_d^{eq} is calculated using the following equations:

$$x_d^{eq} = 0.01 \cdot \left(d_1(T) \cdot \sqrt{p_1} + d_2(T) \cdot p_1 + d_3(T) \cdot \sqrt{p_1^3} \right) \quad (1.29)$$

$$d_1(T) = 0.4874 - \frac{608}{T} + \frac{489530}{T^2} \quad (1.30)$$

$$d_2(T) = -0.060602 + \frac{135.6}{T} - \frac{69200}{T^2} \quad (1.31)$$

$$d_3(T) = 0.00253 - \frac{4.154}{T} + \frac{1509}{T^2} \quad (1.32)$$

where p_1 and T are expressed in MPa and K, respectively.

1.2.3 Crystallization models

de'Michieli Vitturi et al. [31]

The equilibrium volume fraction of crystals (α_c^{eq}) is calculated using Eq. 1.33.

$$\alpha_c^{eq} = \min(\alpha_{c,max}, \alpha_{c,0} + 0.55 \cdot (0.58815 \cdot p^{-0.5226})) \quad (1.33)$$

where $\alpha_{c,max}$ is the maximum crystallinity, $\alpha_{c,0}$ is the initial volume fraction of crystals and $\min()$ is the minimum function.

1.2.4 Outgassing models

Forchheimer's law [3]

The model is dependent on the relative position of the fragmentation level. Below magma fragmentation, since a non-linear relationship between pressure gradient and gas flow rate has been recognized, Degruyter et al. [3] describe the outgassing process using the Forchheimer's law, which includes the influence of viscous (linear term) and inertial forces (quadratic term) (Eq. 1.34). Above magma fragmentation, the model presented by Yoshida and Koyaguchi [32] is considered; and the presence of a transitional domain is also assumed (Eq. 1.34). Please note that $|dp/dz| = \delta_f \cdot \Delta u$.

$$\left| \frac{dp}{dz} \right| = \begin{cases} \frac{\mu_g}{k_D}(\Delta u) + \frac{\rho_g}{k_I}(\Delta u)^2 & \text{if } \alpha_g \leq \alpha_{cr} \\ \left(\frac{\mu_g}{k_D}(\Delta u) + \frac{\rho_g}{k_I}(\Delta u)^2 \right)^{1-t} \cdot \left(\frac{3C_D}{8r_a} \rho_g(\Delta u)^2 \right)^t & \text{if } \alpha_{cr} < \alpha_g < \alpha_t \\ \frac{3C_D}{8r_a} \rho_g(\Delta u)^2 & \text{if } \alpha_g \geq \alpha_t \end{cases} \quad (1.34)$$

where Δu is the velocity difference between both phases, subscript g refers to the exsolved gas phase, C_D is a drag coefficient, r_a is the average size of the fragmented

magma particles, $t = (\alpha_g - \alpha_{cr})/(\alpha_t - \alpha_{cr})$, α_t controls the range of the transitional domain, while k_D and k_I are the Darcian and inertial permeabilities, respectively (Eq. 1.35 and Eq. 1.36).

$$k_D = \frac{(f_{rb}r_b)^2}{8}\alpha_g^m \quad (1.35)$$

$$k_I = \frac{f_{rb}r_b}{f}\alpha_g^{(1+3m)/2} \quad (1.36)$$

$$r_b = \left(\frac{\alpha_g}{\frac{4\pi}{3}N_{bd}\alpha_l} \right)^{1/3} \quad (1.37)$$

where f_{rb} is the throat-bubble size ratio (0.1 - 1), r_b is the average bubble size, N_{bd} is the bubble density number ($10^8 - 10^{16} \text{ m}^3$) and f and m are fitting parameters.

Darcy's law

In this case, the inertial forces below magma fragmentation (quadratic term) and the transitional domain are not considered, and thus the resulting model is described by the following expression:

$$\left| \frac{dp}{dz} \right| = \begin{cases} \frac{\mu_g}{k_D}(\Delta u) & \text{if } \alpha_g \leq \alpha_{cr} \\ \frac{3C_D}{8r_a}\rho_g(\Delta u)^2 & \text{if } \alpha_g > \alpha_{cr} \end{cases} \quad (1.38)$$

1.2.5 Degassing model

If lateral degassing is considered, it follows Eq. 1.39.

$$J_{lat} = \frac{\rho_2\alpha_2k}{\mu_2f_{\epsilon_2}} \frac{\partial p}{\partial r} \Big|_{r=R_{eq}} \quad (1.39)$$

where k is country rocks permeability.

1.2.6 Equations of state

In order to define the specific internal energy and entropy of melt, crystals and dissolved water, a linearized version of the Mie-Gruneisen equation of state [33] was adopted:

$$e_k(\rho_k, T) = \bar{e}_k + c_{v,k}T + \frac{\rho_{0,k}C_{0,k}^2 - \gamma_k p_{0,k}}{\gamma_k \rho_k} \quad (1.40)$$

$$s_k(\rho_k, T) = s_{0,k} + c_{v,k} \cdot \ln \left(\frac{T}{T_{0,k}} \left(\frac{\rho_{0,k}}{\rho_k} \right)^{\gamma_k - 1} \right) \quad (1.41)$$

$$p_k(\rho_k, T) = c_{v,k}(\gamma_k - 1)\rho_k T - \frac{\rho_{0,k}C_{0,k}^2 - \gamma_k p_{0,k}}{\gamma_k} \quad (1.42)$$

where \bar{e}_k is formation energy, $c_{v,k}$ is the specific heat capacity at constant volume, $\rho_{0,k}$ and $C_{0,k}$ are density and sound speed at a reference state, γ_k is the adiabatic exponent and $p_{0,k}$, $s_{0,k}$ and $T_{0,k}$ are pressure, specific entropy and temperature at a reference state. Subscript k refers to melt, dissolved water or crystals.

For the equation of state of exsolved water, two models are available:

Ideal gas

The internal energy, specific entropy and pressure are calculated using equations 1.43, 1.44 and 1.45, respectively.

$$e_g(\rho_g, T) = c_{v,g}T + \bar{e}_g \quad (1.43)$$

$$s_g(\rho_g, T) = c_{v,g} \cdot \ln \left(\frac{T}{T_{0,g}} \left(\frac{\rho_{0,g}}{\rho_g} \right)^{\gamma_g - 1} \right) \quad (1.44)$$

$$p_g(\rho_g, T) = c_{v,g}(\gamma_g - 1) \cdot T \cdot \rho_g \quad (1.45)$$

where $c_{v,g}$ is the specific heat capacity at constant volume, \bar{e}_g is the formation energy, $T_{0,g}$ and $\rho_{0,g}$ are temperature and density at a reference state and γ_g is the adiabatic exponent. Subscript g refers to exsolved gas.

Van der Waals

In this case, we use the following equations:

$$e_g(\rho_g, T) = c_{v,g}T - a \cdot \rho + \bar{e}_g \quad (1.46)$$

$$s_g(\rho_g, T) = c_{v,g} \cdot \ln \left(\frac{T}{T_{0,g}} \left(\frac{\rho_{0,g}}{\rho_g} \cdot (1 - b \cdot \rho_g) \right)^{\gamma_g - 1} \right) \quad (1.47)$$

$$p_g(\rho_g, T) = c_{v,g}(\gamma_g - 1) \cdot T \cdot \frac{\rho_g}{1 - b\rho_g} - a\rho_g^2 \quad (1.48)$$

where:

$$a = \frac{27}{64} \cdot \frac{c_{v,g}^2(\gamma_g - 1)^2 T_{cr,g}^2}{p_{cr,g}} \quad (1.49)$$

$$b = \frac{1}{8} \cdot \frac{c_{v,g}(\gamma_g - 1) T_{cr,g}}{p_{cr,g}} \quad (1.50)$$

1.3 Outputs of the model

MAMMA provides the profiles along the conduit of the following parameters:

- (a) Velocity of both phases.
- (b) Density of both phases.
- (c) Pressure of both phases.
- (d) Temperature.
- (e) Dissolved gas mass fraction and the equilibrium value.
- (f) Exsolved gas volume fraction.
- (g) Crystals volume fraction.
- (h) Mass discharge rate.
- (i) Mixture viscosity.

Bibliography

- [1] E. Romenski, D. Drikakis, and E. Toro. “Conservative models and numerical methods for compressible two-phase flow”. In: *Journal of Scientific Computing* 42.1 (2010), pp. 68–95.
- [2] A. Starostin, A. Barmin, and O. Melnik. “A transient model for explosive and phreatomagmatic eruptions”. In: *Journal of Volcanology and Geothermal Research* 143.1 (2005), pp. 133–151.
- [3] W. Degruyter, O. Bachmann, A. Burgisser, and M. Manga. “The effects of outgassing on the transition between effusive and explosive silicic eruptions”. In: *Earth and Planetary Science Letters* 349 (2012), pp. 161–170.
- [4] A. Costa. “Viscosity of high crystal content melts: dependence on solid fraction”. In: *Geophysical Research Letters* 32.22 (2005).
- [5] C. Cimorelli, A. Costa, S. Mueller, and H.M. Mader. “Rheology of magmas with bimodal crystal size and shape distributions: Insights from analog experiments”. In: *Geochemistry, Geophysics, Geosystems* 12.7 (2011).
- [6] H.M. Mader, E.W. Llewellyn, and S.P. Mueller. “The rheology of two-phase magmas: A review and analysis”. In: *Journal of Volcanology and Geothermal Research* 257.1 (2013), pp. 135–158.
- [7] M. Manga and M. Loewenberg. “Viscosity of magmas containing highly deformable bubbles”. In: *Journal of Volcanology and Geothermal Research* 105.1 (2001), pp. 19–24.
- [8] D.B. Dingwell, N. Bagdassarov, G. Bussod, and S.L. Webb. “Magma rheology”. In: *Mineralogical Association of Canada Short Course Handbook on Experiments at High Pressures and Application to the Earth’s Mantle* 21.1 (1993), pp. 131–196.

-
- [9] A.M. Lejeune and P. Richet. "Rheology of crystal-bearing silicate melts: An experimental study at high viscosities". In: *Journal of Geophysical Research: Solid Earth* 100.B3 (1995), pp. 4215–4229.
- [10] O. Melnik and R.S.J. Sparks. "Nonlinear dynamics of lava dome extrusion". In: *Nature* 402.6757 (1999), pp. 37–41.
- [11] O. Melnik and R.S.J. Sparks. "Controls on conduit magma flow dynamics during lava dome building eruptions". In: *Journal of Geophysical Research: Solid Earth* 110.B2 (2005).
- [12] A. Vona, C. Romano, D.B. Dingwell, and D. Giordano. "The rheology of crystal-bearing basaltic magmas from Stromboli and Etna". In: *Geochimica et Cosmochimica Acta* 75.11 (2011), pp. 3214–3236.
- [13] N.S. Bagdassarov and D.B. Dingwell. "Frequency dependent rheology of vesicular rhyolite". In: *Journal of Geophysical Research: Solid Earth* 98.B4 (1993), pp. 6477–6487.
- [14] A. Costa, O. Melnik, and R.S.J. Sparks. "Controls of conduit geometry and wallrock elasticity on lava dome eruptions". In: *Earth and Planetary Science Letters* 260.1 (2007), pp. 137–151.
- [15] V.C. Ducamp and R. Raj. "Shear and densification of glass powder compacts". In: *Journal of the American Ceramic Society* 72.5 (1989), pp. 798–804.
- [16] H. Eilers. "Die viskosität von emulsionen hochviskoser stoffe als funktion der konzentration". In: *Colloid & Polymer Science* 97.3 (1941), pp. 313–321.
- [17] H. Eilers. "Die viskositäts-konzentrationsabhängigkeit kolloider systeme in organischen lösungsmitteln". In: *Kolloid-Zeitschrift* 102.2 (1943), pp. 154–169.
- [18] J.K. Mackenzie. "Elastic constants of a solid containing spherical holes". In: *Proceedings of the Royal Society B* 63.1 (1950), pp. 2–11.
- [19] S.L. Quane, J.K. Russell, and E.A. Friedlander. "Time scales of compaction in volcanic systems". In: *Geology* 37.5 (2009), pp. 471–474.
- [20] J.O. Sibree. "The viscosity of froth". In: *Transactions of the Faraday Society* 30.1 (1934), pp. 325–331.

- [21] M.N. Rahaman, L. De Jonghe, G.W. Scherer, and R.J. Brook. "Creep and densification during sintering of glass powder compacts". In: *Journal of the American Ceramic Society* 70.10 (1987), pp. 766–774.
- [22] G. Taylor. "The viscosity of a fluid containing small drops of another fluid". In: *Proceedings of the Royal Society of London. Series A, Containing Papers of a Mathematical and Physical Character* 138.834 (1932), pp. 41–48.
- [23] E.W. Llewellyn and M. Manga. "Bubble suspension rheology and implications for conduit flow". In: *Journal of Volcanology and Geothermal Research* 143.1 (2005), pp. 205–217.
- [24] K.U. Hess and D. Dingwell. "Viscosities of hydrous leucogranitic melts: A non-Arrhenian model". In: *American Mineralogist* 81.9-10 (1996), pp. 1297–1300.
- [25] C. Romano, D. Giordano, P. Papale, V. Mincione, D. Dingwell, and M. Rosi. "The dry and hydrous viscosities of alkaline melts from Vesuvius and Phlegrean Fields". In: *Chemical Geology* 202.1 (2003), pp. 23–38.
- [26] D. Giordano, J. Russell, and D. Dingwell. "Viscosity of magmatic liquids: a model". In: *Earth and Planetary Science Letters* 271.1 (2008), pp. 123–134.
- [27] D. Giordano, P. Ardia, C. Romano, D. Dingwell, A. Di Muro, M.W. Schmidt, A. Mangiacapra, and K.U. Hess. "The rheological evolution of alkaline Vesuvius magmas and comparison with alkaline series from the Phlegrean Fields, Etna, Stromboli and Teide". In: *Geochimica et Cosmochimica Acta* 73.21 (2009), pp. 6613–6630.
- [28] A.G. Whittington, B.M. Hellwig, H. Behrens, B. Joachim, A. Stechern, and F. Vetere. "The viscosity of hydrous dacitic liquids: implications for the rheology of evolving silicic magmas". In: *Bulletin of Volcanology* 71.2 (2009), pp. 185–199.
- [29] D. Di Genova, C. Romano, K.U. Hess, A. Vona, B.T. Poe, D. Giordano, D.B. Dingwell, and H. Behrens. "The rheology of peralkaline rhyolites from Pantelleria Island". In: *Journal of Volcanology and Geothermal Research* 249 (2013), pp. 201–216.

-
- [30] Y. Zhang. "H₂O in rhyolitic glasses and melts: measurement, speciation, solubility, and diffusion". In: *Reviews of Geophysics* 37.4 (1999), pp. 493–516.
- [31] M. de'Michieli Vitturi, A.B. Clarke, A. Neri, and B. Voight. "Transient effects of magma ascent dynamics along a geometrically variable dome-feeding conduit". In: *Earth and Planetary Science Letters* 295.3 (2010), pp. 541–553.
- [32] S. Yoshida and T. Koyaguchi. "A new regime of volcanic eruption due to the relative motion between liquid and gas". In: *Journal of Volcanology and Geothermal Research* 89.1 (1999), pp. 303–315.
- [33] O. Le Métayer, J. Massoni, and R. Saurel. "Modelling evaporation fronts with reactive Riemann solvers". In: *Journal of Computational Physics* 205.2 (2005), pp. 567–610.